ELSEVIER

Polymer 40 (1999) 577–587

polymer

Properties of thermoplastic polyurethane elastomers containing liquid crystalline chain extender (I) synthesis and properties of hard segments

Tsai-Fa Hsu, Yu-Der Lee*

Department of Chemical Engineering, National Tsing Hua University, Hsinchu, 300 Taiwan, ROC

Received 9 January 1998; revised 17 April 1998; accepted 30 April 1998

Abstract

Polyurethanes prepared from 1,6-diisocyanate hexane (HDI) and 2,4-tolylene diisocyanate (2,4-TDI) with liquid crystalline chain extender 4,4′-bis(n-hydroxyalkyloxy)biphenyl (*n*-PBP, $n = 2, 3, 6$) were reported. Characterizations of monomers and polymers were performed by infrared spectroscopy (IR), ^{1}H-NMR, solid-state C^{13}-NMR, and elemental analysis. The phase transition behaviors of polyurethanes were investigated by Global TSC, DSC, and polarized microscopy (POM). Our results showed that monomers 4,4′-bis(n-hydroxyalkyloxy) biphenyl exhibit smectic type mesophase. It was observed that the longer the spacer length of polyurethanes, the higher the chain mobility, the larger DOD (degree of disorder) value and the lower the relaxation time. Also the phase transition temperature of polyurethanes decreases with increasing spacer length. DSC measurements and texture observations indicated that H2, H3, H6 and T6 exist in both mesophase and crystal phase. Quantitative analysis of temperature dependence hydrogen bonding revealed that hydrogen bonded content (X_b) of the C=O group for all samples decreased with increasing temperature. For the H series, both X_b and ΔH decrease with increasing spacer length of the mesogenic diol.

Keywords: Thermoplastic polyurethane; Liquid crystalline; Thermal stimulated current

1. Introduction

Liquid crystalline segmented polyurethane elastomer containing mesogenic diols as chain extenders is a new class of thermoplastic elastomers [1–4]. The liquid crystalline hard domains are composed of diisocyanate and mesogenic diol and act as physical cross-links for the network. Since Iimura et al. [5] first reported on liquid crystalline polyurethane (LCPUs), a few studies regarding synthesis and phase transition behavior have appeared in the literature [6–22]. They have shown that LCPUs exhibit both mesophas and crystal phase [8–10] and have extremely high crystallinity upon annealing [11,12]. The phase behavior would also be affected by the formation of hydrogen bonding [13] and different diisocyanate [14]. Recent studies on liquid crystalline polyurethanes elastomers were concentrated on synthesis, phase transition behavior, annealing effect and chain–chain interactions [16–23]. Penczek and coworkers found that 25 mol% of mesogenic component would be sufficient to impart liquid crystalline properties, but LCPUs still exhibit crystalline behavior [15–17].

For polyurethanes, hydrogen bonding may form between the NH group of the urethane group and the carbonyl group and adjacent oxygen atom in the urethane group, as well as the ester carbonyl or ether oxygen of the soft segment. Tanaka revealed that more than 85% of NH groups form hydrogen bonding at room temperature [24]. The absorption bands of both NH and C=O groups are composed of two kinds of vibration, hydrogen bonded and non-hydrogen bonded, namely bonded and free absorption, respectively. The frequency of free absorption bands are higher than those of bonded absorptions for both NH and C=O vibrations. While treated by heat or deformation, the intermolecular interactions of polyurethane may change. So, the absorption bands shift to higher frequencies and change in the shape, half-width and integrated intensity [24–29]. The absorption band would also be affected by the steric factors associated with packing and the frequency shift has been accepted as a measure of the strength of hydrogen bonding [27]. Quantitative analysis of hydrogen bonding and thermodynamic parameters can be estimated via infrared

* Corresponding author.

0032-3861/98/$ - see front matter
PII S0032-3861(98)00331-0

spectroscopy by the following equation [26,27,30,31]:

$$K_d = \frac{(1 - X_b)^2}{X_b} \quad (1)$$

$$K_d = \exp\left(\frac{-\Delta H}{RT} + \frac{\Delta S}{R}\right) \quad (2)$$

where X_b represents hydrogen bonding content and can be obtained from IR measurement under the assumption of Beer's law, and K_d is the equilibrium constant for the dissociation of hydrogen bonded NH group, ΔH is the dissociation enthalpy of hydrogen bonding.

Thermally stimulated current/relaxation map analysis (TSC/RMA) is a powerful instrument which is capable of determining the characteristics of the morphological properties of polymer materials such as glass transitions, phase separation and molecular chain relaxation [32–36]. Furthermore, the RMA spectra obtained from thermal windowing technique can be used to estimate some thermodynamic parameters so as to interpret the molecular chain motion.

In this research, the effects of mesogenic chain extenders, with various spacer lengths, on the properties of polyurethane hard segments were investigated and reported. Polyurethane elastomers containing mesogenic chain extender diols will be reported in an another study.

2. Experimental

2.1. Materials

2-Chloro ethanol and 3-chloro-1-propanol were purchased from Aldrich. 1-Chloro-6-hydroxyhexane was purchased from ACROS. 1,6-Diisocyanate hexane (HDI) and 1,4-butadiol were purchased from TCI and used as received. 4,4′-Biphenol was recrystallized with ethanol before use. 2,4-Tolylene diisocyanate (2,4-TDI) was purchased from Merck and purified by distillation under vacuum. A mixture of NMP and CaH2 was stirred overnight, then distilled under vacuum and stored with a 4-Å molecular sieve.

2.2. Polymerization

Monomers, *n*-PBP (4,4′-bis(n-hydroxyalkyanoxy) biphenyl) were synthesized according to the method described in the literature [12–14], where $n = 2$, 3 and 6, respectively. The synthesis procedures of polyurethanes are in accordance with the method reported by MacKnight et al. [37,38]. In a four-neck round-bottomed flask equipped with mechanical stirrer, additional funnel and condenser, the mixture of 0.02 mol 2-PBP (5.48 g), 0.03 g T-12 and 60 ml NMP was heated to 50°C under nitrogen. Then, 0.02 mol 1,6-diisocyanate hexane (3.36 g) was added slowly. After stirring for 1 h, the temperature was raised to 80°C and maintained for 24 h. The mixture was poured into cold methanol and the white product was filtered and refluxed with methanol for 24 h. After filtering, the product was dried at 80°C under vacuum for 24 h. The synthetic scheme is described in Scheme 1. There were two series of polymers synthesized; codes of the polymers have been abbreviated to HB, HN and TN, where H represents HDI and T stands for TDI, while B is 1,4-butadiol, *n* is the number of *n*-PBP, i.e. 2 for 2-PBP.

2.3. Measurements

Elemental analyses (EA) were carried out on a Perkin-Elmer 2400 C, H, N analyzer. ^{1}H-NMR was performed on a AM-400 NMR instrument with d_6-dimethyl sulfoxide (d_6-DMSO) as the standard. Solid-state C^{13}-NMR was performed on the same instrument. Thermal analyses were performed at a heating rate of 10°C/min under nitrogen atmosphere on a Du Pont 910 DSC/TGA equipped with LNCA cooling system. The textures of mesomorphic

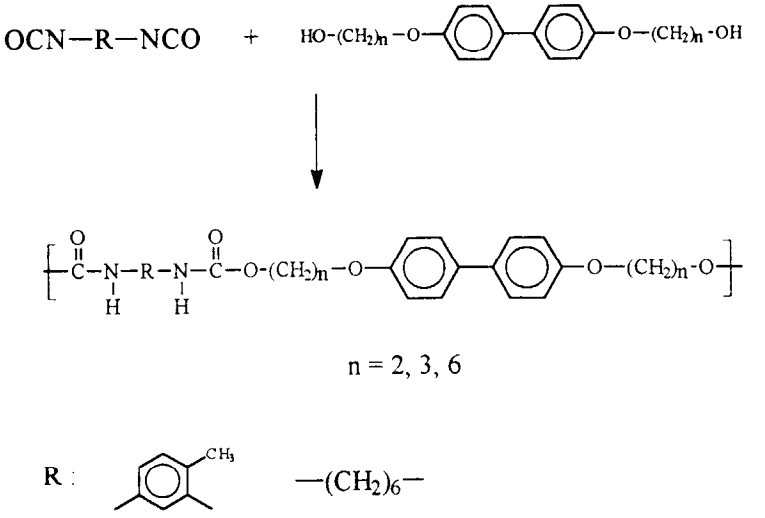

Scheme 1.

phase were observed on a Leitz Polarized Optical Microscope with a THMS600 heating stage. Inherent viscosities were measured with Ubbelhode viscosmeter on 0.5 g/dL in NMP at 30°C.

2.4. Infrared spectroscopy

Typical infrared spectra (IR) were obtained using a Perkin-Elmer 842 infrared spectrometer. The characterization spectra of monomers and polymers were measured by mixing with KBr powder. The investigation of temperature dependence of hydrogen bonding of polymers was measured by casting the samples on a NaCl window with a 10% trifluoroacetic acid solution and being dried at 50°C for 20 min in the oven. With a low boiling temperature, trifluoroacetic acid was used to avoid the annealing effect during the dry process. The complete evaporation of trifluoroacetic acid was confirmed by the absence of COOH group absorption. After evaporating the solvent, another NaCl window was covered and the windows were put into a model equipped with a temperature controller. The model temperature was raised to a set point which is higher than the melting point of the sample and was maintained for 10 min. The absorption infrared spectrum was taken on the cooling scan and the evaluated temperature on the NaCl window's surface was obtained by a TES 1310 thermometer. The scanning range was 4000~400 cm^{-1}, the scan number was 16 and the resolution was 4 cm^{-1}. The raw data were processed with graphic software using the baseline method and Gaussian curve-fitting to calculate the area of both bonded and free absorption bands [24–29].

2.5. Thermal stimulated current and relaxation map analysis (TSC/RMA)

A Solomat TSC/RMA 9100 (Solomat Instruments, Stamford, CT) spectrometer was operated at temperatures ranging from − 100 to 120°C under an electric field ranging from 0 to 500 V/mm. The measurements of Global TSC were carried out as described in a previous study [32]. RMA investigations were performed by thermal windowing of TSC with a 5°C thermal window. Some thermodynamic parameters regarding physical properties such as relaxation time of compensation (τ_c), degree of disorder (DOD) were calculated as follows.

$$\tau(t) = \tau_{0a} \exp\left(\frac{\Delta H}{kt}\right) \tag{3}$$

$$\mathrm{DOD} = 100 - 2 \times [\ln \tau_c + \ln T_c + 23.76] \tag{4}$$

where τ_{0a} is the pre-exponential factor, ΔH is the activation enthalpy, and k is the Boltzmann's constant. DOD of the structure, defined by a single value via Eq. (4), represents the dielectric environment of the bonds. DOD is an important parameter which can be obtained from the E–E plot (ΔS_p versus ΔH_p) by the extrapolated value of the entropy of activation for $\Delta H_p = 0$. It may be considered as the indicator of the degree of orientation of polymer in the amorphous region.

3. Results and discussion

3.1. Characterizations of monomers and polymers

Structural characterizations of monomers measured by IR, EA and ^{1}H-NMR agree well with the prediction. Measurements of EA are listed in Table 1. The infrared spectra of homopolymers are shown in Fig. 1. The N–H absorption band is found at 3500~3300 cm^{-1}, methylene group absorption bands at 2950~2800 cm^{-1}, and C=O at 1780~1640 cm^{-1}. Solid state C^{13}-NMR of H series (includes H2, H3 and H6) are illustrated in Fig. 2. The chemical shift agrees with the structural diagrams. For the H2 sample, the absorption peak A represents the four methylene groups of HDI, peak B is assigned to the end side methylene group connecting the amide group, peak C is assigned to the α carbon in the benzene ring, peak D is assigned to the amide group, and peak E includes other carbons in the benzene ring. The star symbols (*) note the side bands in solid state NMR spectra. The shoulder of peak A (28 ppm) grows gradually to peak G (16 ppm) with the increase of spacer length of mesogen. The distinct separated peak is found in Fig. 2(c) when the spacer length is six. On the other hand, the full width half maximum (FWHM) of peaks reduced with increasing spacer length, as observed in

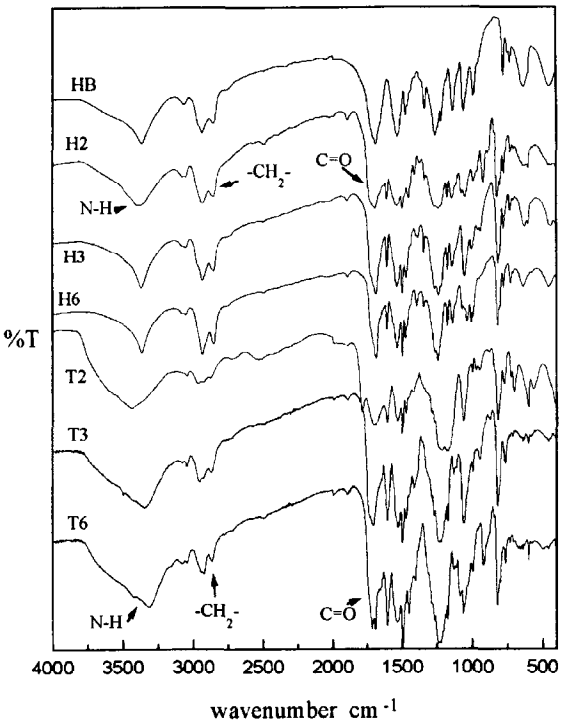

Fig. 1. The infrared spectrums of polyurethanes.

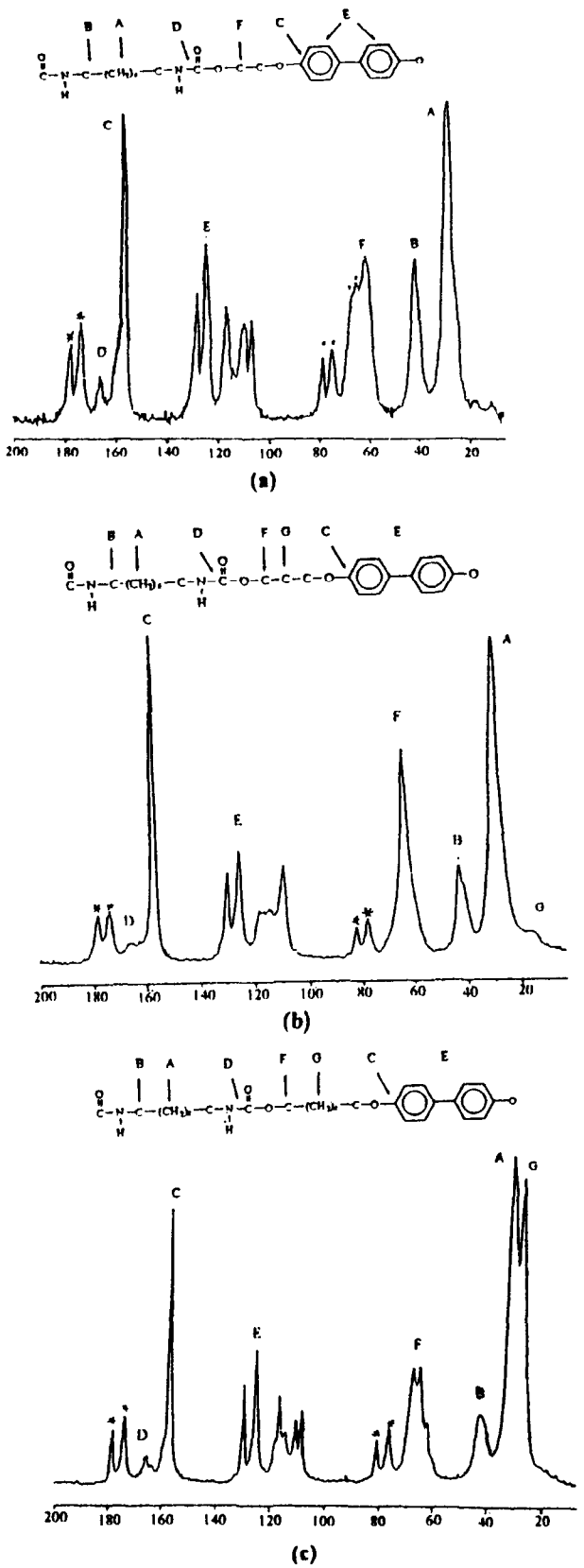

Fig. 2. Solid state C^{13}-NMR spectrums of H series polyurethanes: (a) H2, (b) H3, (c) H6.

Table 1
The properties and characterization of mesogenic diols

Code	Yield (%)	T_m °C	T_i °C	Calculated (%) C	H	O	Found (%) C	H	O
2PBP	86	158	219	70.07	6.57	22.73	69.90	6.62	23.48
3PBP	82	192	214	71.52	7.28	21.20	71.31	7.32	21.37
6PBP	79	99.4	174	74.61	8.81	16.58	74.66	8.78	16.56

Fig. 2. Take peak C (156 ppm) as an example, the FWHM of trace (c) is clearly narrower than that of trace (a). When all the parameters of NMR and the sample are identified, the linewidth (T_2 spin–spin relaxation time) of solid state NMR spectra is determined by molecular motion [39,40]. As seen from Fig. 2, the T_2 relaxation time (linewidth) decreases with the increase in spacer length, indicating the dipole interaction in the long space length is reduced, which also means an increase in molecular motion in long spacer length. This result agrees with the general observation that chain mobility increases and the relaxation time of the carbon atom decreases with increasing spacer length [41–43]. It is worth noting that higher chain mobility, i.e. longer spacer length, encourages the formation of mesophase for liquid crystalline polymers [32] but it also encourages crystallization for semi-crystalline polymers [41,44–47].

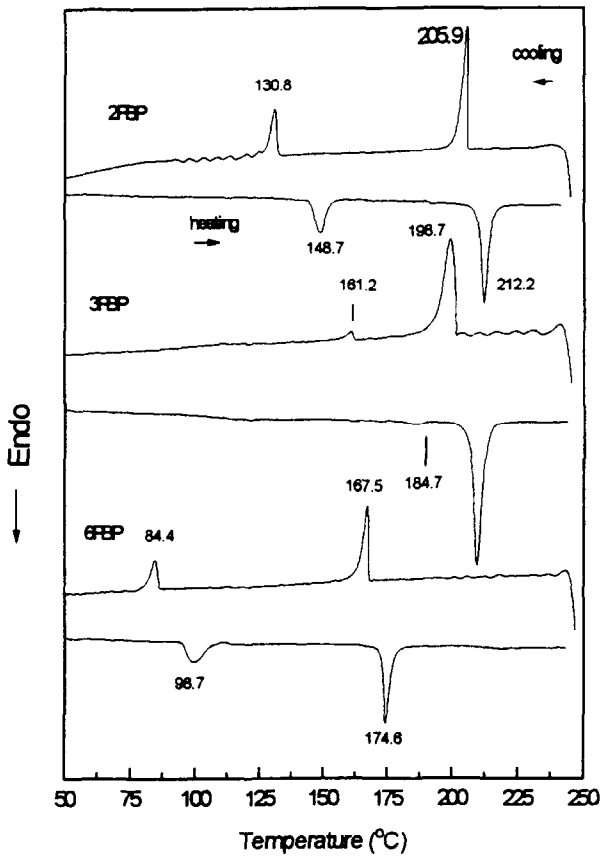

Fig. 3. The phase transition behavior of monomers measured at a heating or cooling rate of 10°C/min, respectively.

Table 2
The properties of polyurethanes hard segments

Code	Yield (%)	T_p (°C)	T_g^a (°C)	T_m (°C)	T_i (°C)	ΔT^b	η_{inh}^c
HB	88.12	50	18.4	165	–	–	0.109
H2	88.76	80	65.7	191.5	208.8	13.3	0.154
H3	87.98	75	61.8	161.7	191.2	29.5	0.242
H6	96.0	70	54.0	165	182	17	0.102
T2	88.9	120	115	256	–	–	0.163
T3	79.43	120	112	160	–	–	0.161
T6	94.33	105	95	139	154	15	0.213

[a]Measured by TSC.
[b]$T = T_i - T_m$.
[c]Measured on a 0.5-dL/g NMP solution at 30°C.

3.2. Phase transition behavior

3.2.1. Monomers

The phase transition behaviors of mesogenic monomers investigated by DSC are illustrated in Fig. 3. All the DSC thermograms of monomers show two endothermic peaks on the heating scan and two exothermic peaks on the cooling scan, which demonstrate enantiotropic liquid crystalline behavior. Both the melting temperature (T_m) and the isotroplization temperature (T_i) of monomers decrease with increasing spacer length. Monomers might create an odd–even effect but we cannot show it here because of the lack of more information. As shown in Fig. 4, the X-ray diffraction spectra of monomers show distinctive characteristic peaks at small angles (less than 7°) indicating possible smectic mesophase. The d-spacing at small angles is 15.22Å for 2-PBP ($2\theta = 5.8°$), 17.31 Å for 3-PBP ($2\theta = 5.1°$) and 23.85 Å for 6-PBP ($2\theta = 3.7°$).

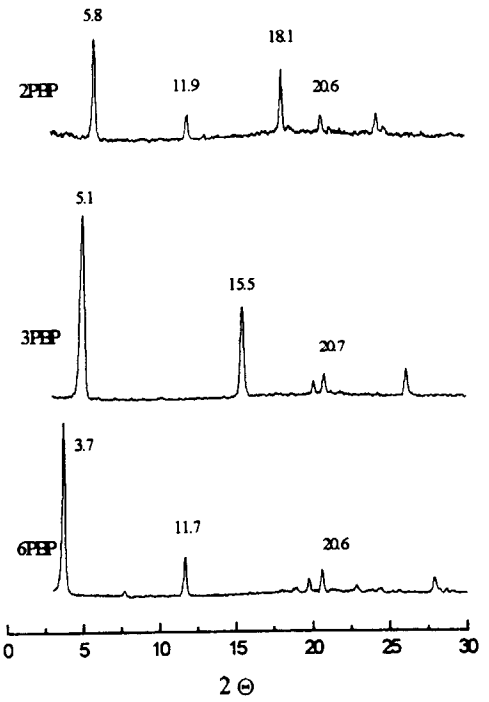

Fig. 4. X-ray spectra of monomers measured at room temperature.

It is clear that the d-spacing increases with increasing length of the spacer. These smectic liquid crystalline textures of monomers were further verified by polarized microscope, as shown in Fig. 5.

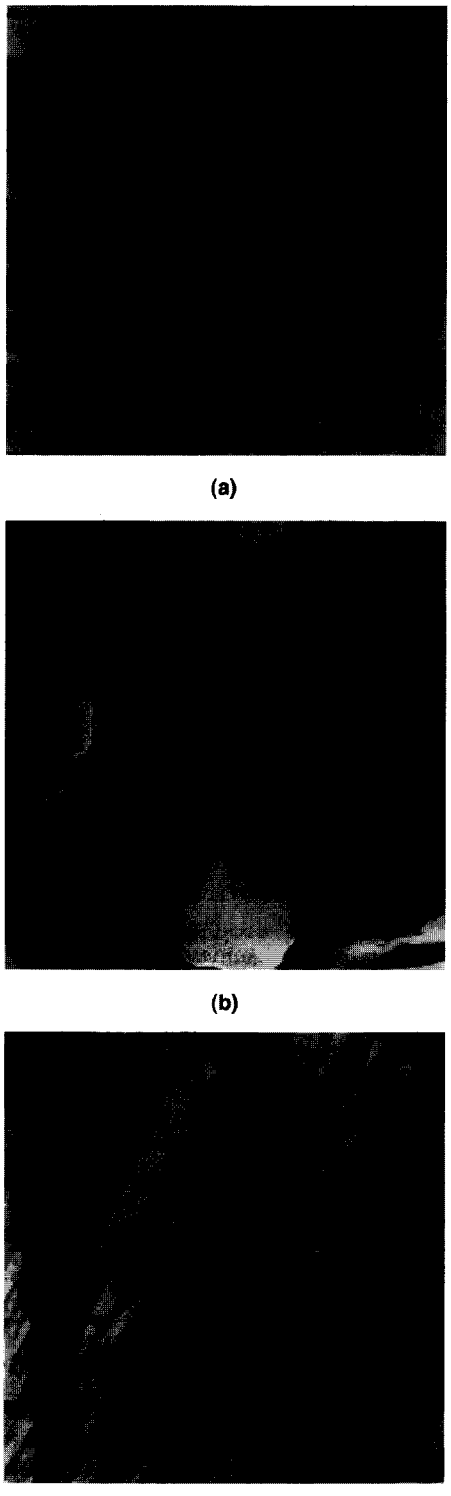

Fig. 5. Liquid crystalline textures of monomers: (a) 2-PBP, 180°C, 200 × ; (b) 3-PBP, 200°C, 200 × ; (c) 6-PBP, 170°C, 200 × .

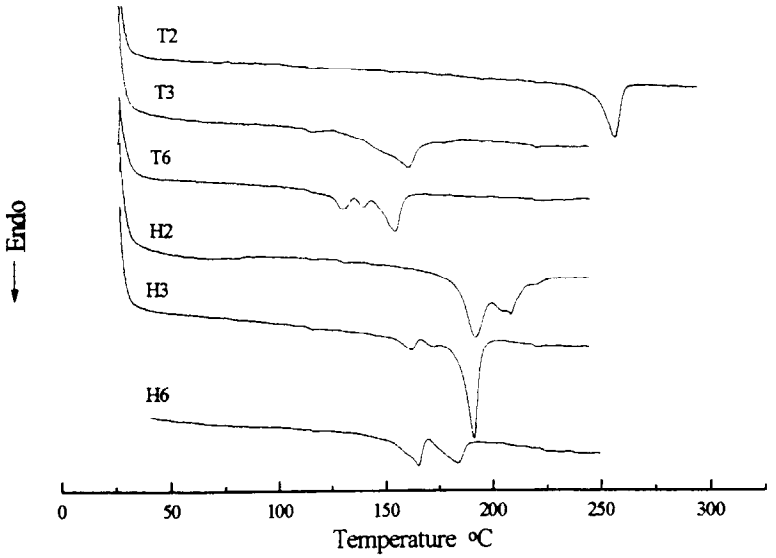

Fig. 6. DSC thermograms of H and T series measured at a heating rate of 10°C/min.

3.2.2. Polymers

DSC thermograms of polymers H and T series are illustrated in Fig. 6 and Table 2. Upon heating, H2, H3 and H6 show two distinct endothermic peaks, evidence of the existence of mesophase. Owing to the changes of chain mobility, the phase transition temperature of H series decreases with increasing spacer length. Besides the spacer length of mesogen, the phase transition behavior of H series is also affected by the conformation of six methylene groups of HDI [28] and the biphenyl moiety [13]. According to the mechanism of relaxation of a few methylene groups ($n \geq 4$) in amorphous presented by Schaztki, MacKnight proposed three sequential structures of the methylene sequence [28]. For HDI only, the N–C bond acts as the rotation axis for the methylene sequence and it is presumed that the NH groups are fixed by intermolecular hydrogen bonds [28]. In addition, MacKnight revealed that the six methylene spacer is in *trans* conformation and the biphenyl moiety orientates with its plane at 51° with respect to the all-*trans* hexamethylene plane which results in the biphenyl moieties tending to have a layer structure [13]. Therefore, H6 with longer spacer length and higher chain mobility has a phase transition temperature lower than H3 but also shows a narrow mesophase temperature range (Table 2). The morphological observations of the H series performed by POM and X-ray diffraction spectra indicated the coexistence of nematic mesophase and crystal phase (Fig. 7).

Phase transition behaviors of T series polyurethanes are shown in Fig. 6 as well. Upon heating, the DSC thermograms of both T2 and T3 show a single endothermic peak while the tracer of T6 shows three endothermic peaks. The T_m of the T series also decrease with increasing spacer length. Because of the more rigid TDI moiety and intermolecular hydrogen bonding, spacer lengths of 2 and 3 are not long enough to form mesophase [17,19–21]. A crystal–crystal transition of T6 is observed at approximately

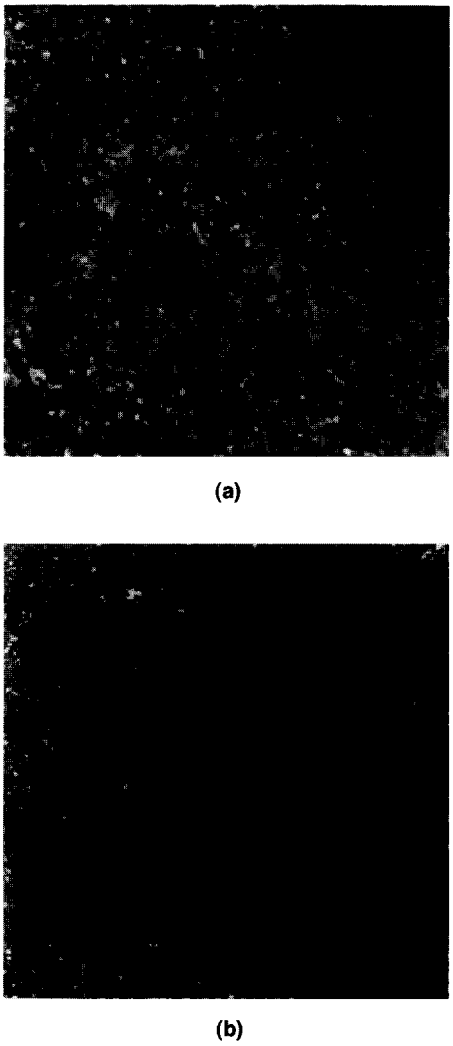

Fig. 7. Liquid crystalline textures of polyurethanes: (a) H6, 178°C, 200 × (b) T6, 145°C, 200 × .

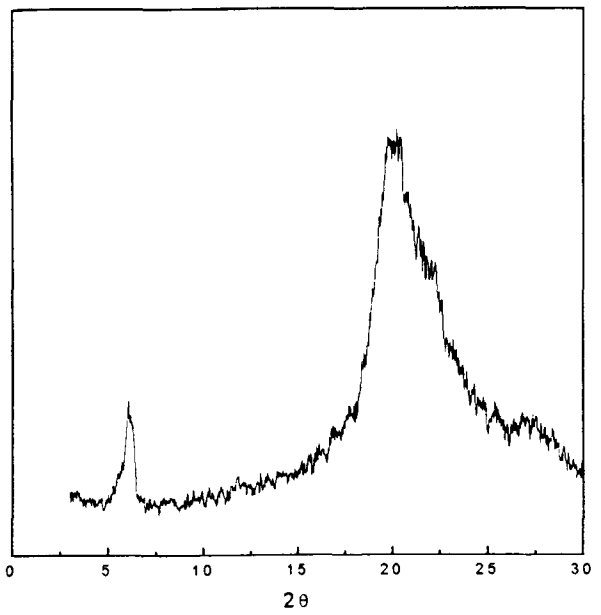

Fig. 8. The X-ray diffraction pattern of T6 quenched from molten state.

129°C followed by two endothermic peaks at 139 and 154°C, corresponding to melting (T_m) and isotropic temperature (T_i), respectively. As evidence, in the X-ray diffraction pattern of the quenched sample, shown in Fig. 8, T6 exhibits both smectic mesophase and crystal phase.

3.3. Global TSC

The glass transition temperatures (T_g) of the H series which are not distinct in the DSC thermograms can be measured by global TSC. The polarized temperature (T_p) is set to be about 15–20°C higher than T_g. The polarized temperature (T_p) and T_g of the H and T series are given in Table 3. As shown in Fig. 9, the temperature at the maximum peak intensity represents the glass transition temperature (T_g). The outcomes of TSC show that the glass transition temperature of both H and T series decrease with increasing spacer length of the mesogen. Comparing the T_gs of the H and T series with similar spacer lengths, the T_gs of the T series are higher than those of the H series because TDI is more rigid than HDI, as shown in Table 2.

3.4. RMA

We have already manifested the fact via C^{13}-NMR that longer spacer length with higher chain mobility results in less chain order. Such a phenomenon can be further verified by the RMA measurements and compensation search with a 5°C thermal window. The first freeze temperature (T_0) of the thermal windowing method is about 40°C lower than T_g and the final depolarization temperature (T_f) is 10°C higher than T_g. Fig. 10 shows the thermal windows of TSC for the H series. The shapes of TSC thermal windows become more symmetric as the spacer length increases, as seen in Fig.

Table 3
The Eyring table of H series polyurethanes hard segments

Code	T_c (°C)	log τ_c (s)	r^2	DOD
HB	216.5	− 7.449	0.9972	74.41
H2	177.1	− 3.413	0.9971	56.26
H3	149.9	− 5.991	0.9979	68.18
H6	222.8	− 6.814	0.9984	71.63

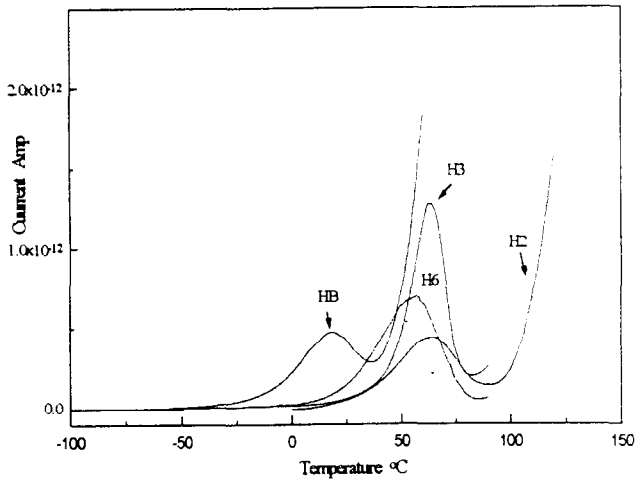

Fig. 9. TSC spectra of H series polyurethanes.

Table 4
Changes in the degree of hydrogen bonding and equilibrium constant with temperature

HB			H2		
Temperature (°C)	X_b	K_d	Temperature (°C)	X_b	K_d
40	0.931	0.00511	31	0.895	0.0124
50	0.925	0.00608	62	0.836	0.0322
75	0.914	0.00809	95	0.834	0.0329
95	0.874	0.0181	123	0.832	0.0335
127	0.831	0.0343	143	0.828	0.0353
150	0.774	0.0659	165	0.753	0.0807
167	0.685	0.145	185	0.734	0.0906
H3			H6		
37	0.653	0.185	30	0.565	0.335
55	0.647	0.200	55	0.503	0.492
75	0.622	0.230	65	0.497	0.509
100	0.592	0.281	80	0.470	0.597
130	0.580	0.304	100	0.441	0.708
150	0.564	0.338	140	0.407	0.862
171	0.563	0.340	165	0.375	1.042
T6					
32	0.870	0.0194			
38	0.852	0.0257			
58	0.842	0.0296			
80	0.824	0.0376			
111	0.819	0.0400			
140	0.812	0.0435			
186	0.803	0.0483			

10(b, c). The height of partial polarization TSC peaks of HB are higher than the others. Following the Arrhenius relationship shown in Eq. (3), the relaxation map (RMA) of the H series was obtained from the plots of ln t versus T^{-1} and illustrated in Fig. 11. Each diagram shows a different shape of the Arrhenius line set which represents the fingerprint of the polymer. The slope and intercept of the Arrhenius line are the activation enthalpy and entropy, respectively.

Owing to the fact that the activation entropy is affected by the polarized temperature, the DOD value is used as an indicator of entropy in RMA measurement. The compensation point (T_c, τ_c) which represents the mutual coupling characterization among different relaxation modes is obtained from the results of RMA via compensation search and is used to calculate the DOD value. The outcomes of compensation search shown in Table 3 indicate that the DOD values of H2, H3 and H6 increase with increasing spacer length, but are lower than that of HB. This suggests that polyurethanes containing a mesogen unit have higher orientation than polyurethane without mesogen, while the orientation decreases with increasing spacer length [32].

3.5. Temperature dependence of hydrogen bonding

The C=O absorption band is used to carry out the quantitative analysis of hydrogen bonding because the distinct free absorption band of the C=O group is easy to be observed. The variations of the C=O group's absorption band with respect to temperature for H3 and H6 are shown in Fig. 12. Survey IR spectra did not show any evidence of solvent. A strong absorption band observed at 1690 cm^{-1} is assigned to the hydrogen bonded C=O group absorption while a shoulder found at 1720 cm^{-1} corresponds to the free C=O group absorption. When the temperature is increased, the intensity of the hydrogen bonded band decreases. However, the intensity of the shoulder, i.e. the free absorption band, increases with increasing temperature.

Prior to the quantitative analysis of hydrogen bonding, all C=O absorption bands were fitted by Gaussian function. The integrated area (A_b) and the height of the hydrogen bonded peaks decrease while the area (A_f) and height of the free absorption bands increase with increasing temperature. The placements of both free and bonded peaks shift gradually towards higher frequencies

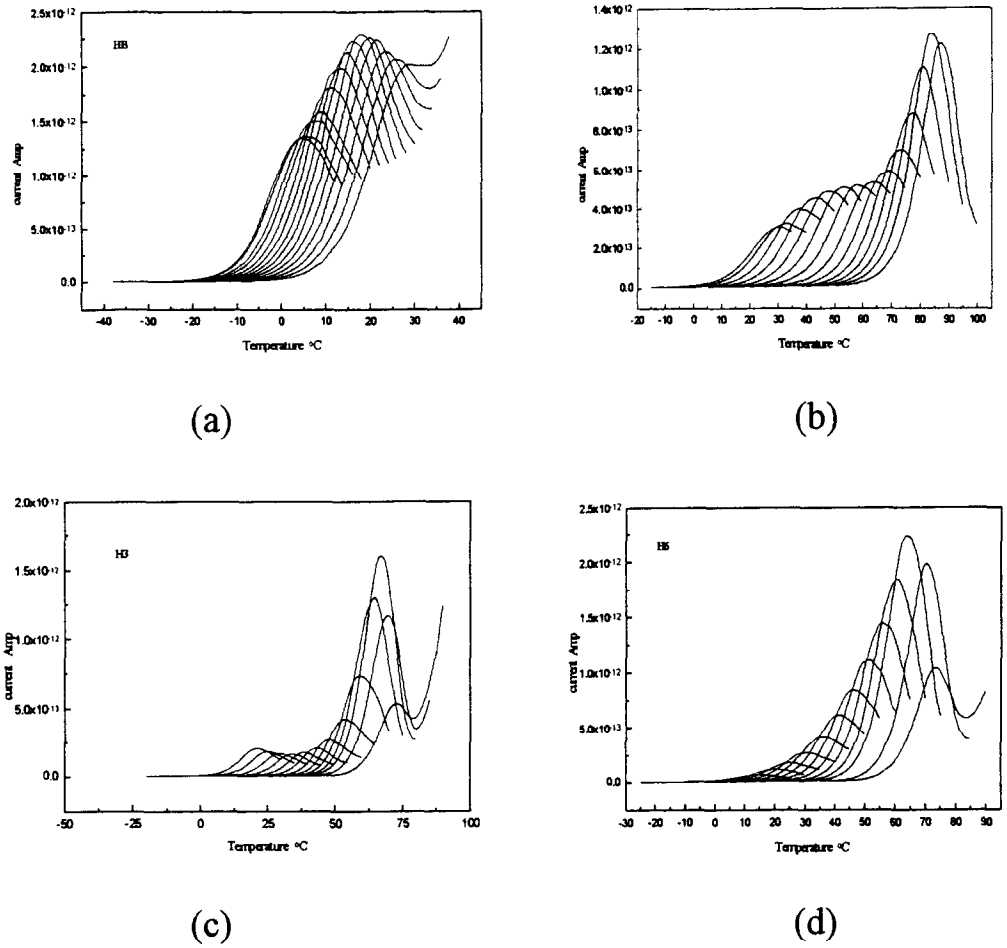

Fig. 10. Thermal-windows of H series polyurethanes: (a) HB; (b) H2; (c) H3; (d) H6.

and the half-width ($W_{1/2}$) increases with increasing temperature. The fraction of the hydrogen bonded C=O group (X_b) can be estimated by the following equation [30,31]:

$$X_b = \frac{A_{bonded}}{A_{bonded} + A_{free} \times 1.7} \quad (5)$$

The equilibrium constant of dissociation of hydrogen bonded C=O group (K_d) was obtained via Eq. (1) Eq. (2) and the calculated values of X_b and K_d are listed in Table 4. The plots of X_b versus temperature are shown in Fig. 13. For H6, a nearly linear decreasing relationship was found between 65 and 165°C. Because the relationship between X_b and phase transition temperature is still not clear [26,29–31], it is suggested that a discontinuous point observed at 55°C might correspond to T_g which is close to both the DSC and TSC investigations (54°C). Similar transitions were found in other plots. The X_b of H2 and T6 decrease slightly with temperatures above T_g but H2 shows a distinct decrease at 165°C. For the H series, the longer the spacer length, the lower the X_b observed. As the spacer length is 6, the X_b of H6 is lower than that of T6.

As shown in Fig. 14, the plots of $-\ln K_d$ versus T^{-1} demonstrate that the equilibrium constant K_d increases with increasing temperature and shows similar transitions to those observed in Fig. 13. It can also be found that K_d increases with increasing spacer length. In Table 4, the difference in X_b between H3 and H6 is smaller than that between H2 and H3 suggesting that the chain mobility of H6 is affected by hydrogen bonding.

4. Conclusion

Liquid crystalline polyurethanes containing mesogenic diols with various spacer lengths were prepared with different diisocyanates, i.e. HDI, 2,4-TDI and 4,4′-bis(n-hydroxyalkyloxy)biphenyl (n-PBP, n = 2, 3, 6). The mesogenic diols characterized by DSC, POM and X-ray diffraction show a smectic enantiotropic mesophase and the phase transition temperatures decrease with increasing spacer length. Results from C^{13}-NMR, RMA and DSC analyses indicate that the chain mobility of H series polyurethanes increase with increasing spacer length while the T_m and T_i of polyurethanes decreased. According to the results of X-ray diffraction patterns and POM photographs, H2, H3, H6 and T6 exist both in crystal phase and different types of mesophase. Moreover, the phase transition behavior was affected by

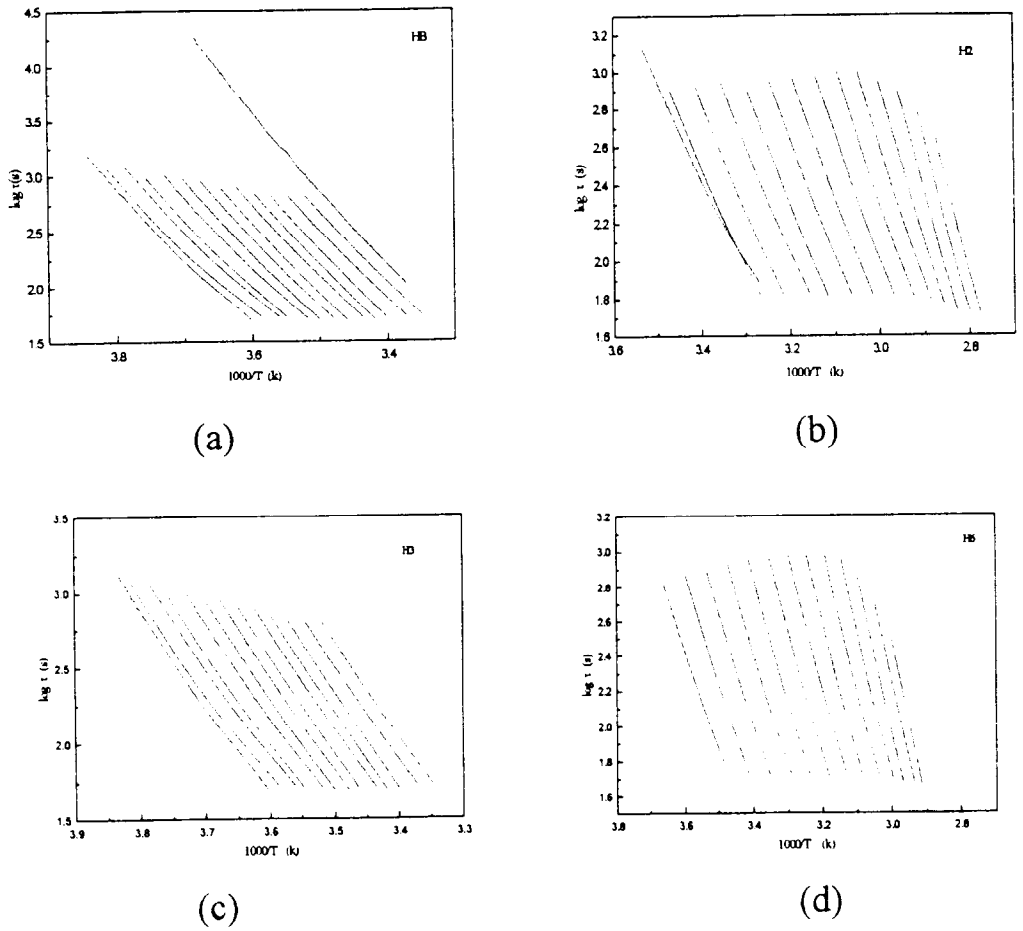

Fig. 11. Map (RMA) of H series polyurethanes.

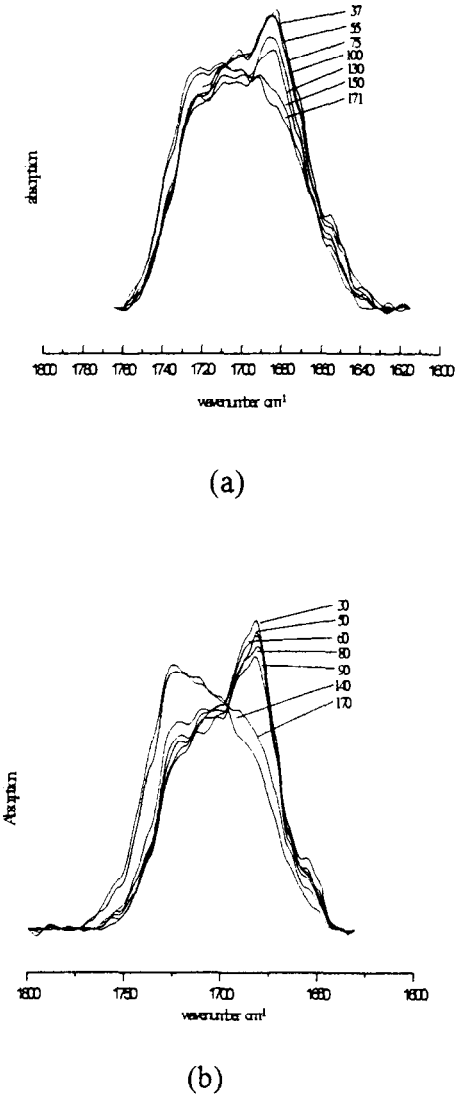

Fig. 12. The temperature dependence of C=O group absorption: (a); H3 (b) H6.

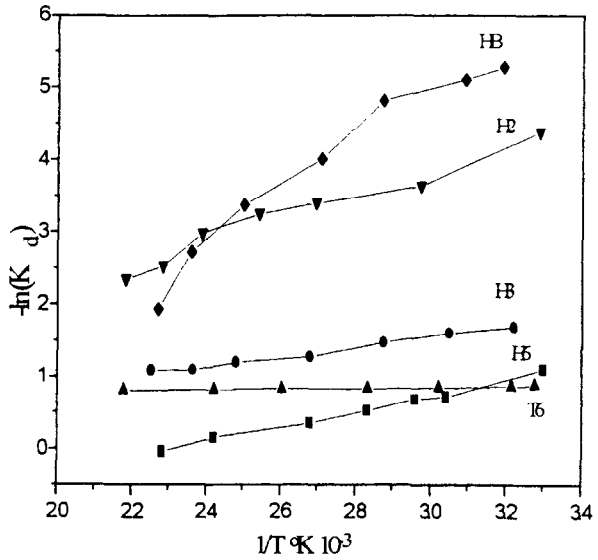

Fig. 14. Temperature variation of the hydrogen bonding equilibrium constant of polyurethanes.

hydrogen bonding. Through quantitative analysis of temperature dependence, hydrogen bonding was obtained via IR spectroscopy. It shows that hydrogen bonding content (X_b) decreases with increasing spacer length. Without a mesogen, HB has a higher X_b but lower orientation while the XB and orientation of H2, H3 and H6 are affected by the spacer length.

Acknowledgements

The authors gratefully acknowledge the financial support from the National Science Council of Republic of China (NSC 87-2216-E-007-024).

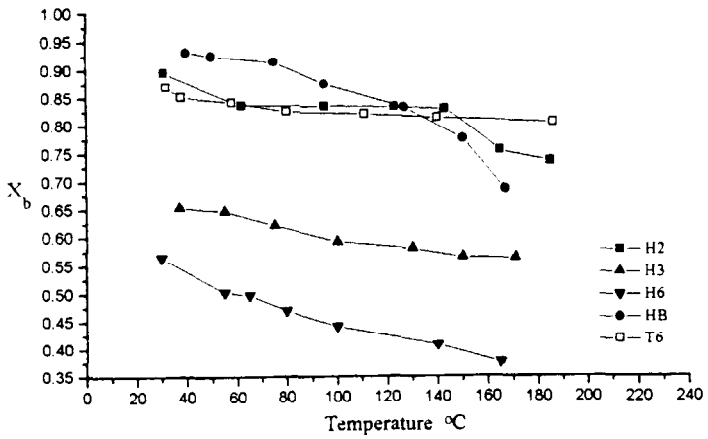

Fig. 13. Plots of the fraction of hydrogen bonded C=O (X_b) versus temperature.

References

[1] Tang W, Farris RJ, MacKnight WJ, Eisenbach CD. Macromolecules 1994;27:2814.
[2] Wedler W, Tang W, Winter HH, MacKnight WJ, Farris RJ. Macromolecules 1995;28:512.
[3] Tang W, MacKnight WJ, Hsu SL. Macromolecules 1995;28: 4284.
[4] He X, Jia X, Yu X. J Apply Polym Sci 1994;54:207.
[5] Iimura K, Koide N, Tanabe H, Takeda M. Makromol Chem 1981;182:2569.
[6] Tanaka M, Nakaya T. Makromol Chem 1986;187:2345.
[7] Smith GW. Molecular crystals and liquid crystals, vol. 180, Iss PB, 1990:201.
[8] Mormann W, Baharifar A. Polymer Bulletin 1990;24(4):413.
[9] Tanaka M, Nakaya T, Macro J. Sci Chem 1989;A26(12):1655.
[10] Mormann W, Brahm M. Macromolecules 1991;24(5):1096.
[11] Stenhouse PJ, Valles EM, Kantor SW, MacKnight WJ. Macromolecules 1989;22:1467.
[12] Pollack SK, Shen DY, Hsu SL, Wang Q, Stidham HD. Macromolecules 1989;22:551.
[13] Papadimitrakopoulos F, Hsu SL, MacKnight WJ. Macromolecules 1992;25:4671.
[14] Papadimitrakopoulos F, Sawa E, MacKnight WJ. Macromolecules 1992;25:4682.
[15] Smyth G, Valles EM, Pollack SK, Grebowicx J, Stenhoues PJ, Hsu SL, MacKnight WJ. Macromolecules 1990;23:3389.
[16] Pollack SK, Shen DY, Hsu SL, Wang Q, Stidham HD. Macromolecules 1989;22:551.
[17] Papadimitrakopoulos E, Kantor SW, MacKnight WJ. Polym Prepr 1990;31(1):486.
[18] Back Lee J, Kato T, Yoshida T, Uryu T. Macromolecules 1993;26 (19):4989.
[19] Penczek P, Frich KC, Szczepaniak B, Rudnik E. J Polym Sci Polym Chem 1993;31:1211.
[20] Szczepaniak B, Frich KC, Penczek P, Rudnik E, Cholinska M. J Polym Sci Polym Chem 1993;31:3231.
[21] Szczepaniak B, Frich KC, Penczek P, Mejsner J, Leszzynska I, Rudnik E. J Polym Sci Polym Chem 1993;31:3223.
[22] Tang W, Farris RJ, MacKnight WJ, Eisenbach CD. Macromolecules 1994;27:2814.
[23] He X, Jia X, Yu X. J Appli Polym Sci 1994;54:207.
[24] Seymou RW, Estes GM, Cooper SL. Macromolecules 1970;3 (5):579.
[25] Paik Sung CS, Smith TW. Macromolecules 1980;13:117.
[26] Paik Sung CS, Schneider NS. Macromolecules 1977;10(2):452.
[27] Brunette CM, Hsu SL, Cooper SL. Macromolecules 1982;3(5):71.
[28] Koberstain T, Gancarz I. J Polym Sci, Polym Phys 1986;24:2487.
[29] MacKnight WJ, Yang M. J Polym Sci Sympo 1973; No. 14:817.
[30] Senich CA, MacKnight WJ. Macromolecules 1980;13:106.
[31] Coleman MM, Lee KH, Skrovanek DJ, Painter PC. Macromolecules 1986;19:2149.
[32] Liu S-F, Lee Y-D. J Polym Sci, Polym Phys 1995;33:133.
[33] Ibar J.P. Polym Eng Sci 1991;31(20):1467.
[34] Sauer BB, Hsiao BS. J Polym Sci, Polym Phys 1993;31:917.
[35] Vaia RA, Sauer BB, Tse OK, Giannelis EP. J Polym Sci, Polym Phys 1997;35:59.
[36] Dias AB, Moura Ramos JJ. Polymer 1994;35(6):1253.
[37] Tang W, Farris RJ, MacKnight WJ. Macromolesules 1994;27:2814.
[38] Wedler W, Tang W, Henning Winter H, MacKnight WJ, Farris RJ. Macromolecules 1995;28:512.
[39] Mehring M. Principles of high resolution NMR is solid state. Berlin: Springer Verlag, 1983.
[40] Komoroski RA. High resolution NMR spectroscopy of synthetic polymer in bulk. FL: VCH, 1986:Ch. 7.
[41] Tang W, MacKnight WJ, Hsu SL. Macromolecules 1995;28:4284.
[42] Zhang X, Takegoshi K, Kunio H. Macromolecules 1992;25:2336.
[43] Zhang X, Shimoda M, Toyoda A. J Polym Sci Part B: Polym Phys 1994;32:1399.
[44] McBrierty VJ, Zhang X, Douglass DC, Zhang JX, Jerome R. Polymer 1994;35:3811.
[45] Sun SJ, Hsu KY, Chang TC. J Polym Sci Polym Chem 1995;33:787.
[46] Kajiyama T, MacKnight WJ. Macromolecules 1969;2(3):254.
[47] MacKnight WJ, Yang M. J Polym Sci Symposium 1973;42:817.